The Investigations of Fe$_2$MnGe Heusler Alloy Using Density Functional Theory

KONRAD GRUSZKA*

Institute of Physics, Faculty of Production Engineering and Materials Technology, Czestochowa University of Technology, 19 Armii Krajowej Str., 42-200 Czêstochowa, Poland

The paper presents results of computational studies on Fe$_2$MnGe heusler alloy using density functional theory approach. The material exhibit half metalic properties with spin polarization of 98% in the Fermi energy. Paper contain results of three population analysis methods namely Löwdin's, Henkelman (Bader) and Yu and Trinkle (YT) using Quantum Espresso, Critic2 and Bader Charge Analysis sowtware packages. The charge density visualization planes resulting from Bader analysis are also presented. Studies showed localized-covalent bonding character between transition metals and Ge. The total magnetization is caused mainly by to Mn-d shell electrons, with small Fe and marginal Ge magnetic moments participation.

Keywords: density functional theory, population analysis, charge density, Heusler alloys

Fundamental research of new materials is very important for bringing understanding of their properties in relation to their atomic and electronic structures. Development of new techniques and methods that allow for deep insight into materials properties at their lowest level is crucial for progress in manufacturing technology as well as for their basic interpretation. For this reason methods like molecular mechanics (MM) [1,2], molecular dynamics (MD) [3,5], density functional theory (DFT) [6,9], Hartree-Fock (HF) [10-12], or quantum monte carlo (QMC) [13-16] to name few, and also many other *ab initio* approaches has gained recently great interest. With the use of those methods, one can obtain information that is normally not available or at least very difficult to obtain using other experimental techniques. One example is to illustrate the behaviour of electrons in crystalline phases. Techniques like x-ray diffraction/scattering can be utilised to obtain information about electron clouds density in material, but averaged over the whole crystal, so for example the particular effect of single vacancy defect on electron density is therefore lost or strongly diluted. On the other hand, *first principles* simulation methods allow for studying behaviour of individual electrons if required, therefore enabling much more information about considered material.

The Fe$_2$MnGe material is one of the Heusler's kind compound characterized by the X$_2$YZ type structure. This material exhibits magnetocaloric effect [17] and is a competitor to othe magnetocaloric materials i.e. La(Fe,Si)$_{13}$- type alloys [18,19]. Moreover, it could be applied in spin injector devices [20]. Such material can be laboratory produced using long term heat treatment of polycrystalline ingot, possibly Bridgeman or Czochralski traditional methods. This particular material crystallize in the L2$_1$ structure, in cubic Fm-3m space group (no. 225) where the Mn atoms occupy corners and faces of the cube, Ge occupies middle of the edges and Fe is located inside, interpenetrating with the second cube (Fe occupy the corners). Previously we reported the electronic and magnetic properties study focusing mainly on the influence of iron-copper ion substitution in relation to half metallic properties [21-29]. As we shown earlier, this substitution

breaks the high spin polarization at Fermi level, so the material properties are gaining more metallic character. In this paper main focus is devoted to structural and binding study unravelling its characteristics by the use of density functional theory calculations using Quantum Espresso software and various bonding and charge population analysis.

Experimental part
Computational details
All DFT calculations presented here were performed using Quantum Espresso software package with the additional use of Critic2 code [30, 31] (for both Bader and Yu and Trinkle (YT) analysis) and Bader charge analysis code [32, 33] for comparison purpose. As in previous study a projected augmented-wave (PAW) pseudopotentials including scalar relativistic effects and nonlinear core corrections were used. The electronic configuration of Mn was [Ne] 3s^2 3p^6 4s^2 3d^5 located in *4a*, Ge - [Ar] 4s^2 3d^{10} 4p^2 in *4b* and Fe - [Ne] 4s^2 3d^6 in *8c* Wyckoff positions. The generalized gradient approximation (GGA) approach in the Perdew, Burke and Ernzerhof (PBE) [33, 34] form was used. In contrast to previous calculations the supercell approach was not necessary, as this time no substitutions were made. Because of this reduction, the convergence tests were carried out again. The Brillouin zone sampling with appropriate Monkhorst-Pack grid was done with 15 x 15 x 15 k-points. For structure optimization the Broyden-Fletcher-Goldfarb-Shannon (BFGS) algorithm was utilized with force criteria set to 10^{-3} Ry/au. The kinetic energy cutoff ecutwfc=80 Ry and ecutrho=800 Ry for charge density cutoff. The electronic convergence criteria was set to 10^{-8} Ry. As we shown in [21, 34-36] and our previous paper ferromagnetic configuration was the most stable one, therefore only this kind of magnetic ordering was included in the calculation, as it has some noticeable influence on structural parameters. For the population analysis the 72 x 72 x 72 FFT-grid was used in Bader charge code and in Critic2 code. For charge analysis first a cube file was generated consisting of 300 x 300 x 300 electronic density points via postprocessing tools (pp.x) provided by Quantum Espresso package.

* email: kgruszka@wip.pcz.pl

Results and discussions
Structural parameters

In order to verify the correctness of calculations comparison between some structural parameters to previous studies were made. Figure 1 shows structure of
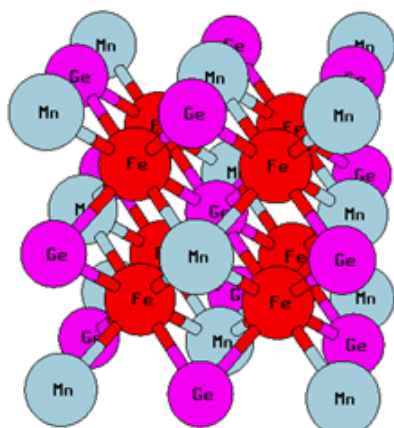
Fig. 1. Structure of conventional unit cell for Fe$_2$MnGe material

Fe$_2$MnGe material and some structural parameters are presented in table 1.

By analysing data collected in table 1, a very good accordance with previous work as well as with experimental results can be seen. Therefore conclusion about correctness of adopted methodology can be stated. Next, the charge population calculations were made.

Charge density and population analysis

In order to get some insight into binding and magnetic properties several population analysis were performed table 2 shows Lowdin charge population analysis data (the plane-waves states of valence electrons are being projected on the psudo-atomic basis and the sum of these projections or Löwdin charge).

Values given in table 2 are showed taking into account only valence electrons (including 3s and 3p semicore states for both Mn and Fe). As can be seen by analysing Löwdin data, the valence iron charge is less than 16, which is normal Fe behaviour, as Fe tends to give electrons to the more electronegative neighbours (in this case germanium electronegativity is 2.01 in respect to iron's 1.83). The same

Structure	a [A]	V [A³]	Fe-Fe* [A]	Fe-Ge [A]**	Fe-Mn [A]***	Mn-Mn [A]****
Fe₂MnGe – this work	5.691	184.32	2.845	2.464	2.464	4.023
Fe₂MnGe - FM mag.- previous work [19]	5.689	184.13	2.844			
Fe₂MnGe [32]	5.682	-	-			
Fe₂MnGe [33]	5.700	-	-			
Fe₂MnGe [34] - EXP.	5.781	193.21	-			

Table 1
STRUCTURAL PARAMETERS

* nearest Fe-Fe; **Fe to central Ge; *** nearest Fe-Mn; ****nearest Mn-Mn

Atom	Total charge	s	p	d
Fe	**15.6895**	**2.5789**	**5.9961**	**7.1145**
	Spin up	s = 1.2821	p = 2.9981 pz= 0.9994 px= 0.9994 py= 0.9994	d = 3.6891 dz2= 0.7358 dxz= 0.7392 dyz= 0.7392 dx2-y2= 0.7358 dxy= 0.7392
	Spin down	s = 1.2968	p = 2.9980 pz= 0.9993 px= 0.9993 py= 0.9993	d = 3.4254 dz2= 0.5310 dxz= 0.7878 dyz= 0.7878 dx2-y2= 0.5310 dxy= 0.7878
polarization	**0.2489**	**s = -0.0148**	**p = 0.0001**	**d = 0.2637**
Ge	**14.6348**	**1.3974**	**3.2393**	**9.9980**
	Spin up	s = 0.7060	p = 1.5786 pz= 0.5262 px= 0.5262 py= 0.5262	d = 4.9990 dz2= 0.9999 dxz= 0.9997 dyz= 0.9997 dx2-y2= 0.9999 dxy= 0.9997
	Spin down	s = 0.6914	p = 1.6608 pz= 0.5536 px= 0.5536 py= 0.5536	d = 4.9990 dz2= 0.9999 dxz= 0.9997 dyz= 0.9997 dx2-y2= 0.9999 dxy= 0.9997
polarization	**-0.0676**	**s = 0.0146**	**p = -0.0822**	**d = 0.0000**
Mn	**14.4910**	**2.6997**	**5.9959**	**4.2242**
	Spin up	s = 1.3606	p = 2.9981 pz= 0.9994 px= 0.9994 py= 0.9994	dz2= 0.9706 dxz= 0.7610 dyz= 0.7610 dx2-y2= 0.9706 dxy= 0.7610
	Spin down	s = 1.3391	p = 2.9979 pz= 0.9993 px= 0.9993 py= 0.9993	d = 1.5712 dz2= 0.1378 dxz= 0.4318 dyz= 0.4318 dx2-y2= 0.1378 dxy= 0.4318
polarization	**2.6746**	**s = 0.0214**	**p = 0.0002**	**d = 2.6530**

Table 2
LOWDIN VALENCE CHARGES PROJECTED ON ATOMIC ORBITALS

Atom	Löwdin charge	Bader charge (critic2)	Bader charge (bader code)	YT charge
Fe	15.648	16.172	16.172	16.166
Mn	14.635	14.070	14.070	14.099
Ge	14.490	14.586	14.586	14.568

situation is visible for Mn valence charge, which is lower (starting configuration is 15). The iron 4s shell charge is only $\sigma=0.58$ therefore iron tends to lose its least bonded electrons. Calculation of magnetic properties (in terms of magnetic moment localized on each atom) reveals that iron ions have only small contribution to the overall cell's magnetism and the Ge ions are negligible in this sense. The Fe-d subshell is filled with 7 electrons, leaving only 3 unpaired ones, thus reducing its overall spin magnetism (polarization of d orbital is only ~0.26) and giving total Fe magnetic moment of ~0.25 μB. As shown before, the manganese is mainly responsible for materials magnetic properties with 2.67 μB moment resulting mainly from 3d-subshell electrons and the total magnetic moment is ~3 μB. Interestingly, Mn also loses its 4s electrons but in contrast to Fe, it loses its 3d subshell charge, however, its polarization remains high because charge depletion is visible mainly in minority spin channel. The calculated magnetic moments of Ge -0.06 μB, therefore calculated magnetic properties are consistent with other studies. The total charge derived from Löwdin analysis (especially when comparing to other population analysis methods) shows some substantial difference (table 3).

The biggest one is observed at Fe ion population where according to Löwdin analysis charge is not only smaller, but also difference between valence and obtained charge value has opposite sign than those calculated by Bader and Yu-Trinkle methods.

The bader population analysis gives information resulting from analysis of critical points in electron density, and it is usually considered more robust. While analyzing data in table 3 it can be noticed that both Bader charge and YT charge gave very similar results. According to this, it can be concluded that iron tend to gain very small charge Δn_{Fe}~-0.17, germanium charge remains almost constant (bader Δn_{Ge}~-0.07 and YT Δn_{Ge}~-0.1) while Mn noticeably loses charge Δn_{Mn}~0.43 (Δn is calculated as free atom valence charge – calculated charge). However, it should be remembered that observed discrepancies arise from different ways of their evaluation. Nevertheless, from all analysis it seems that Mn tend to lose charge while Ge is an acceptor in this context which is generally expected behavior.
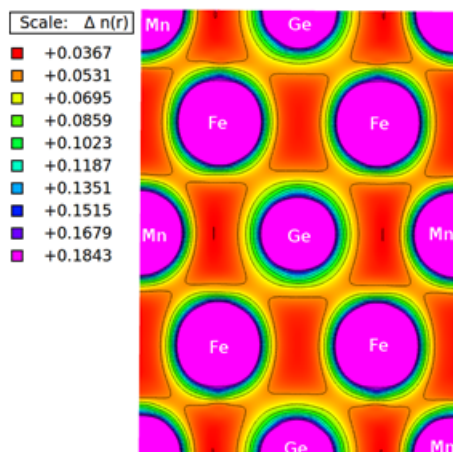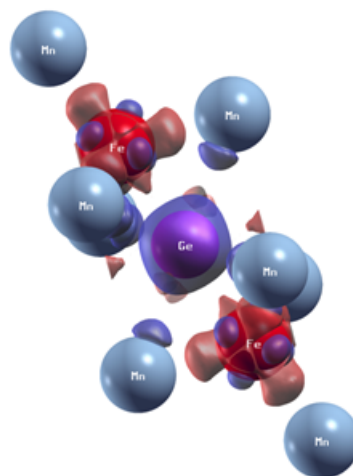
Fig. 3. Charge density minus superposition of atomic densities. In red - positive values, blue- negative values of charge difference

Charge density plot and charge density minus superposition of atomic densities plot are given in figure 2 and figure 3 respectively.

The presented charge distribution for Fe$_2$MnGe shows that character of bonding between central germanium and neighbouring Fe ions is clearly localized, similarly electronic density localization between Fe and Mn ions is visible. In the latter case both density and charge volume between ions seems to be smaller than former, suggesting more localized binding. At the same time, a minimum charge distribution is visible between Fe-Fe ions. Further information about bonding can be derived from charge difference plot (fig. 3). As can be seen there are visible red regions of increased density coming from Fe ions toward Mn. The shape and spatial position of those regions shows significant similarity to sp^3-like orbital hybridization. Also the spherical depletion of charge around germanium is visible, in accordance with data in table 2, where for Ge 4s – shell charge is also depleted.

The bonding type between Fe-Ge and Mn-Ge appear to be a covalent one. This and also band gap in minority channel of total dos [21] suggest that a relatively strong p-d hybridization between both transition metals and germanium occur. As shown in [38, 39] for the covalent like system, the depth of the pseudogap correspond to the strength of the covalent bond. Therefore deeper pseudogap is an indication of stronger hybridization between the electronic orbitals, what corresponds to a stronger covalent bond.

Conclusions

In this paper a Fe$_2$MnGe Heusler alloy was investigated using density functional theory calculations. Structural parameters calculated in this work are in good agreement with both previous studies and experimental results. The various charge population analyses were proposed, namely Löwdin, Bader and Yu-Tinkle methods were utilized, accompanied with charge density plots. Based on obtained results and their analysis, localized bonding picture between transition metals and Ge is emerging. The total magnetization is caused mainly by to Mn-d shell electrons, with small Fe and marginal Ge magnetic moments participation. Both codes (Henkelman and Critic2) gave similar results of valence charge as opposed to Löwdin analysis. The character of bonding between germanium

Fig. 2. Charge density in Mn-Fe-Ge-Fe-Mn (on diagonal) plane. Scale unit electrons/bohr³

and transition metals is covalent, resulting from p-d orbitals hybridization.

References

1.YANG, Q., TO, A.C., Journal of Computational Physics, **336**, 2017, p. 212. https://doi.org/10.1016/j.jcp.2017.01.058.

2.MIRPARIZI, M., ASKI, F., Propulsion and Power Research, **5**, No. 3, 2016, p. 250, https://doi.org/10.1016/j.jppr.2016.07.006.

3.ADJAOUD, O., ALBE, K., Acta Materialia, **145**, 2018, p. 322, https://doi.org/10.1016/j.actamat.2017.12.014.

4.ZHANG, J., WANG, X., ZHU, Y., SHI, T., TANG, Z., LI, M., LIAO, G., Computational Materials Science, **143**, 2018, p. 248, https://doi.org/10.1016/j.commatsci.2017.11.011

5.ZHANG, H., YUAN, S., SUN, J., LIU, J., LI, H., DU, N., HOU, W., Journal of Colloid and Interface Science, **506**, 2017, p. 227, https://doi.org/10.1016/j.jcis.2017.07.042.

6.PIASECKI, M., BRIK, M.G., BARCHIY, I.E., OZGA, K., KITYK, I.V., EL-NAGGAR, A.M., ALBASSAM, A.A., MALAKHOVSKAYA, T.A., LAKSHMINARAYANA, G., Journal of Alloys and Compounds, **710**, 2017, p. 600, https://doi.org/10.1016/j.jallcom.2017.03.280.

7.GRUSZKA, K., NABIA³EK, M., NOGA, T., Archives of Metallurgy and Materials, **61**, No 1, p. 369,   DOI10.1515/amm-2016-0068

8.JIAO, H., ZHAO, K., MA, L., BIAN, T., MA, Y., TANG, Y., Materials Science and Engineering: B, **229**, 2018, p. 184, https://doi.org/10.1016/j.mseb.2017.12.035.

9.ALAY-E-ABBAS, S.M., NAZIR, S., COTTENIER, S., SHAUKAT, A., Scientific Reports, **7**, 2017, Article number: 8439, DOI10.1038/s41598-017-08189-2

10.LOPEZ-QUELLE, M., MARCOS, S., NIEMBRO, R., SAVUSHKIN, L.N., Nuclear Physics A, 971, 2018, p. 149. https://doi.org/10.1016/j.nuclphysa.2018.01.012

11.YOUNG, T.D., VARGAS, R., GARZA, J., Physics Letters A, **380**, No. 5–6, 2016, p. 712,.https://doi.org/10.1016/j.physleta.2015.11.021.

12.CAVALIERE, F., DE GIOVANNINI, U., Physica E: Low-dimensional Systems and Nanostructures, **42**, No. 3, 2010, p. 606.

13.BUENDÍA, E., CABALLERO, M.A., GÁLVEZ, F.J., Chemical Physics Letters, **693**, 2018, p. 72. https://doi.org/10.1016/j.cplett.2018.01.004.

14.NASIRI, S., ZAHEDI, M., Chemical Physics Letters, **634**, 2015, p. 101. https://doi.org/10.1016/j.cplett.2015.05.071.

15.BLUMER, N., KALINOWSKI, E., Physica B: Condensed Matter, **359–361**, 2005, p. 648. https://doi.org/10.1016/j.physb.2005.01.179.

16.CHANDLER BENNETT, M., KULAHLIOGLU, A.H., MITAS, L., Chemical Physics Letters, **667**, 2017, p. 74, https://doi.org/10.1016/j.cplett.2016.11.032.

17.AZAR, S.M., HAMAD, B.A., KHALIFEH, J.M., J.Magn. Magn Mater., **324**, 2012, p. 1776.

18.P. GEBARA, J. KOVAC, Mater. Des., **129**, 2017, p. 111.

19.GÊBARA, P., PAWLIK, P., HASIAK, M., J. Magn. Magn. Mater., **422**, 2017, p. 61.

20.GUEZLANE, M., BAAZIZ, H., HAJ HASSAN, F.E., CHARIFI, Z., DJABALLAH, Y., J. Magn. Magn. Mater., **414**, 2016, p. 219.

21.GRUSZKA, K., SZOTA, M., NABIA³EK, M., Rev. Chim.(Bucharest), **68**, no. 3, 2017, p. 487.

22.JEZ, K., European Journal of Materials Science and Engineering, **3**, no. 1, 2018, p. 3.

23.SANDU, A.V., CIOMAGA, A., NEMTOI, G., BEJINARIU, C., SANDU, I., Journal of Optoelectronics and Advanced Materials, **14**, no. 7-8, 2012, p. 704.

24.JEZ, B., NABIALEK, M., GRUSZKA K., PIETRUSIEWICZ, P., JEZ, K., RZACKI, J., SZOTA, M., BLOCH, K., GONDRO, J., European Journal of Materials Science and Engineering, **2**, no. 2-3, 2017, p. 57.

25.NABIALEK, M., JEZ, B., European Journal of Materials Science and Engineering, **2**, no. 1, 2017, p. 33.

26.BUZEA, C.G., BEJINARIU, C., BORIS, C., VIZUREANU, P., AGOP, M., International Journal of Nonlinear Sciences and Numerical Simulation, **10**, no. 11-12, 2009, p. 1399.

27.STOLERIU, S., IOVAN, G., PANCU, G., GEORGESCU, A., SANDU, A.V., ANDRIAN, S., Mat. Plast., **51**, no. 2, 2014, p. 162.

28.TUGUI, C.A., NEJNERU, C., GALUSCA, D.G., PERJU, M.C., AXINTE, M., CIMPOESU, N., VIZUREANU, P., Journal of Optoelectronics and Advanced Materials, **17**, no. 11-12, 2015, p. 1855.

29.SANDU, A.V., BEJINARIU, C., NEMTOI, G., SANDU, I.G., VIZUREANU, P., IONITA, I., BACIU, C., Rev. Chim. (Bucharest), **64**, no. 8, 2013, p. 825.

30.OTERO-DE-LA-ROZA, A., JOHNSON, E.R., LUAÑA, V., Comput. Phys. Commun, **185**, 2014, p. 1007.

31.OTERO-DE-LA-ROZA, A., BLANCO, M.A., MARTÍN PENDÁS, A., LUAÑA, V., Comput. Phys. Commun. 180, 2009, p. 157.

32.TANG, W., SANVILLE, E., HENKELMAN, G. , J. Phys.: Condens. Matter, **21**, 2009, p. 084204.

33.SANVILLE, E., KENNY, S.D., SMITH, R., HENKELMAN, G., J. Comp. Chem., **28**, 2007, p. 899.

34.J.P. PERDEW, K. BURKE, M. ERNZERHOF, Phys. rev. lett., **77**, 1996, p. 3865. https://doi.org/10.1103/PhysRevLett.78.1396

35.KUMAR V., JAIN, VISHAL JAIN, N. LAKSHMI, K. VENUGOPALAN, AIP Conf. Proc., **1591**, 2014, p. 1130.

36.HAMAD, B., CHARIFI, Z. BAAZIZ, H., SOYALP, F., J. Magn. Magn. Mater., **324**, 2012, p. 3345.

37.L. ZHANG, E. BRUCK, O. TEGUS, K.H.J. BUSCHOW, F.R. DE BOER, J. Alloy. Compd., **352**, No. 1-2, 2003, p.99.

38.XU, J.-H., OGUCHI, T., FREEMAN, A.J., Phys. Rev. B., **36**, 1987, p. 4186, DOI:https://doi.org/10.1103/PhysRevB.36.4186

39.HU, Q.M., YANG, R., XU, D.S., HAO, Y.L. LI, D., WU, W.T., Phys. Rev. B., **68**, 2003, p. 054102, DOI:https://doi.org/10.1103/PhysRevB.68.054102